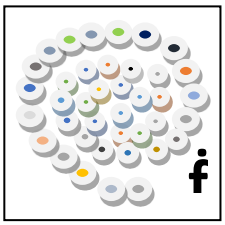

International Journal of Mathematical Analysis and Modelling

(Formerly Journal of the Nigerian Society for Mathematical Biology)

Volume 5, Issue 1 (May), 2022

ISSN (Print): 2682 - 5694
ISSN (Online): 2682 - 5708

International Journal of Mathematical Analysis and Modelling
Volume 5, Issue 1, May 2022, Pages 1 – 17

A mathematical study of effect of constriction and extra cellular matrix gel on aqueous humor flow and IOP

B. A. Ngwu[*†], C. O. Mmaduakor[*], O. E. Abolarin[*], O. A. Akintunde[*], M. Iorkua[‡], and S.U. Isienyi[§]

Abstract

Increase in Intraocular Pressure (IOP) in the eye has been pointed out as a primary risk factor for Glaucoma and; Glaucoma is a leading cause of sight loss globally. Despite this knowledge, the site where this increase in pressure occurs is still under studies. The junction between the endothelia-cell wall of the Schlemn's canal and the juxtacanalicular tissue is known to contain funnel shaped pores which are surrounded by extra cellular matrix gel. The flow of Aqueous Humour through these pores generates a funneling effect (which can be considered as a flow through constricted channel) on the TM. Furthermore, the extra cellular matrix may (exert) contribute some force on the flow dynamics, in the form of drag to Aqueous Humour flow. This study investigated the combined effect of the pores and extra cellular matrix gel (as a drag force) on Aqueous Humour flow dynamics such as Aqueous Humour flow resistance, and hydraulic conductivity respectively. Our results show that these structures affect the flow resistance and hydraulic conductivity, and might likely contribute to increase in IOP.

Keywords: constricted channel flow; constriction and drag; aqueous humuor flow; intraocular pressure; hydraulic conductivity and resistance.

1. Introduction

Aqueous humor (AH) is a fluid in the eyes secreted through ciliary process which leaves through the trabecular meshwork [9]. The conventional outflow route comprises of the trabecular meshwork (TM), the juxtacanalicular connective tissue (JCT), the endothelial lining of Schlemm's canal (SC)

[*] Department of Mathematics, Federal University, Oye-Ekiti, Ekiti State, Nigeria
[†] Corresponding Author: benitho.ngwu@fuoye.edu.ng; benamaobi@gmail.com
[‡] Department of Statistics, Benue State Polytechnic, Ugbokolo, Benue State, Nigeria
[§] Department of Mathematics/Statistics, Akanu Ibiam Federal Polytechnic, Unwana, Afikpo, Nigeria

and the Schlemm's canal (SC) itself [20,29]. As a fenestrated beams and sheets of extra cellular matrix (ECM) covered with endothelial-like cells (TM), the TM is adjacent to SC. Its primary function is to regulate the bulk of the AH outflow from the anterior chamber [32], thereby controlling the intraocular pressure (IOP). The junction between the innermost portion of the TM and the inner wall endothelium cells of SC is the JCT [32]. Extracellular matrix has been discovered in the cells of the TM beams, JCT and SC inner wall of the eye. Basement and stromal ECM are found in the TM beams and JCT region [1]. The TM beam cells which have discontinuous tight junction strands in addition to possessing gap junctions is known to cover the ECM [6, 18,25]. ECM is implicated in outflow resistance because it is critical in maintaining outflow resistance [1] despite that it seems more likely a candidate for the outflow resistance [22]. The SC cells and the JCT ECM are also considered to be responsible for the maintenance of AH outflow resistance. The inner wall cells of the SC have some pores that make funneling possible [18] which creates a hydrostatic effect on the outflow facility [20]. The ECM has a role in the outflow facility of AH as it is primarily thought to cause AH outflow resistance [12, 15, 20, 21, 24, 30], because the ECM and the inner wall cells of SC provides outflow resistance [1] and contribute and control the final the pressure drop by forcing funneling through SC cellular pores [32]. Despite being a candidate for causing outflow resistance, the ECM plays a role also in regulating outflow activity and maintaining IOP. About 25 to 30 pores of the SC which serve as collector channels should allow free circumferential flow of AH but due to segmental flow witnessed in some eyes the fluids do not flow freely, as expected [11, 17, 19].This outflow resistance destabilizes IOP homeostasis which its loss is clearly central to the progression of glaucoma [13, 32]. Glaucoma results from an increase in the resistance of the aqueous humor outflow, which in turn elevates the intraocular pressure (IOP) [31, 33]. Because of this reason it will not be out of place to study the combined effect of these players on AH flow dynamics. See [16, 20, 24] for details.

Earlier, some mathematical works have looked at this problem through different perspectives. These works include [3] that carried out a study of flow of aqueous humor in Schlemm's canal in the eye. They treated the canal segment along which the aqueous humor flows as an elliptic narrow tube. Further, they considered that the inner endothelial wall in contacts with TM is porous and collapsible, and that the inner wall of the SC is deformable as well. By considering that the same quantity of aqueous humor drains through each collector channel is somehow unrealistic. In 2008, Fitt A.D, (2008) [14] also carried a similar study on the SC to determine its influence on Primary open angle glaucoma (POAG). In the study, he considered the flow of aqueous humor from the anterior chamber through the TM into the SC. This he did using lubrication theory. After a study of the flow dynamics of the AH through the iris-lens channel, David M. Silver and Harry A. Quigley, (2004) [10] agrees that there is a pressure difference between the posterior and anterior chambers. In 2018, the circulation of AH through its route is considered as a flow with constriction in a channel [23]. The authors considered the funneling effect as a constriction in the channel of flow. By adjusting the stenosis length and other flow parameters they established that the stenosis length and height has a significant effect on the flow dynamics. Other works that studied the dynamics of the AH outflow activity and its effect on IOP include [2, 4, 5]. These works motivated us to extend [23] by incorporating into the flow a drag force term representing the effect of the ECM gel on the flow dynamics, which, to the best of our knowledge, has not been carried out on the AH flow dynamics. Therefore we here try to investigate the effect of constriction (due to the funneling effect of the SC) and ECM (considered as a form of drag force on the flow dynamic) on the AH flow through the TM and SC.

For ease of communication and understanding, we splited the paper into four sections. The first section is the introduction where a background of the study is presented in addition to review of some related literatures to the work. The definition of the problem and its model equations follows from the second section. In this section is contained some of the assumptions guiding the study with some explanations. The third section is where the mathematical analysis of the model is carried out before the last section. This last section takes care of the numerical results, findings from the work and its conclusion.

2. Definition and model formulation

Here we consider the flow of AH in the eye as a flow through constriction with drag. Consider that at the point of interest (i.e. the junction between the JCT and the inner wall of SC) the channel is a cylindrical tube with stenosis, which is mild and symmetric. In addition, there is a drag force opposing the outflow of AH through the JCT since it is assumed embedded in the ECM and open on the surface. The flow channel is such that fluid (AH in this case) enters through the point z = 0 and continues until it gets to the mouth of the stenosis at z = d where the funneling effect starts. Within the constricted region the flow is steady and continues until the point z = d + l after which the flow profile fills the non-constricted region. But on getting to z = d +3.5l, the effect of the gel manifests thereby causing a drag on the flow velocity. The flow through the ECM (we represented the ECM with the circle in red) is represented by an arrow around the circular region in the channel and signifies nothing but the effect of drag on the flow profile. This is to sya that there is no tangential flow. In doing so, we have assumed a one dimensional flow with a very low convective momentum. In addition, we assumed that the relationship between the axial velocity and axial direction is not significant. This is because of the nature of the channel and the fluid under consideration here. The geometry of flow channel is considered as shown in figure 1.

R is the radius of the free channel, R_δ is the radius of the constricted part of the channel, δ is the radius of constriction, L is the length of the channel, a is the radius of the drag-free channel, R_a is the radius of the drag-filled channel, d is the distance between the entrance and the constriction and L is the length of the constriction.

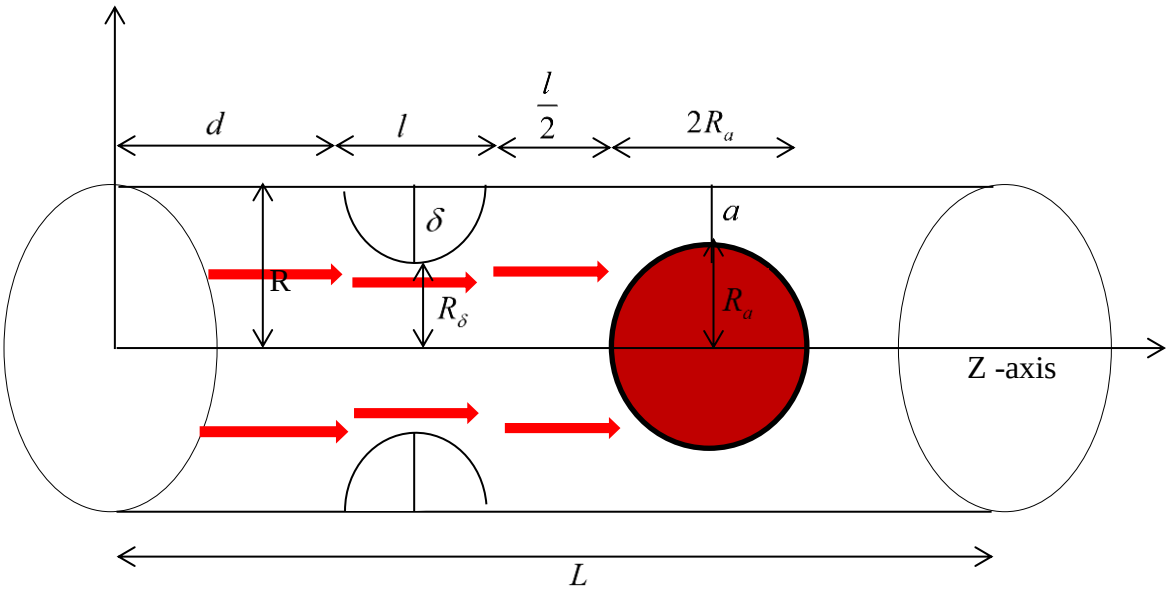

Figure 1. Geometry of the flow channel.

2.1. Model formulation

The equations governing the geometry of the flow channel is defined as presented in equations (1) and (2) respectively.

$$\frac{R_\delta}{R} = \begin{cases} 1-\dfrac{2\delta}{Rl}(z-d); & d \le z \le d+\dfrac{l}{2} \\ 1-\dfrac{\delta}{2R}\left[1+\cos\dfrac{2\pi}{l}\left(z-d-\dfrac{l}{2}\right)\right]; & d+\dfrac{l}{2} \le z \le d+l \end{cases} \tag{1}$$

$$\frac{R_a}{R} = \begin{cases} 1-\dfrac{a}{Rl_a}(z-d_a); & d_a \le z \le d_a+\dfrac{l_a}{2} \\ 1-\dfrac{a}{2R}\left[1+\cos\dfrac{2\pi}{l_a}\left(z-d_a-\dfrac{l_a}{2}\right)\right]; & d_a+\dfrac{l_a}{2} \le z \le d+l_a \\ 1 & \text{otherwise} \end{cases} \tag{2}$$

In the light of the above, the equation governing the AH flow in this case is given by

$$\rho\frac{D\overline{U}}{Dt} = -\overline{\nabla}P + \mu\overline{\nabla}^2 U + \bar{f}$$

where $\overline{U} = (u_1, u_2, u_3)$ is the velocity of the flow, $\frac{D\overline{U}}{Dt}$ is the instantaneous accelerations, $\overline{\nabla}P$ is the pressure gradient, i.e. the pressure drop across the channel length of flow and $\bar{f}$ is the external body force. Since there is no external body, $\bar{f} = 0$. (The aqueous flow is driven by the pressure drop in the channel, which is the difference between the flow at the entrance and exit of the channel). We shall assume that $(u_1, u_2, u_3) = (u_1, 0, 0)$, which is to say that there is only flow along the channel. This in other words means that we consider only a one dimensional flow system. Because of the funneling effect on aqueous flow caused by the JCT on the inner wall of the SC, the dynamics of the flow is considered as a flow with constriction.

Suppose that the channel of flow is such that the point z = d is the end of the hydrodynamic entrance region where the flow stooped developing. Because of this, we shall assume that the flow is fully developed having travelled through the entrance length where the flow was developing. As a result of this, we consider the equations governing the flow (see [23, 27]) to be

$$\frac{\mu}{r}\frac{\partial}{\partial r}\left[r\frac{\partial U}{\partial r}\right] = P_x, \tag{3}$$

$$U(R) = 0, \tag{4}$$

$$U(R_\delta) = \frac{-R_\delta\sqrt{D_a}}{\alpha}U_\delta, \tag{5}$$

$$\frac{\partial U(R_a)}{\partial r} = U_\delta - U_a, \tag{6}$$

where U_δ is the slip velocity at the stenosis and $U_a = -\pi r\mu U$ is the drag velocity due to ECM.

2.2. Analysis of the Problem

We obtain the slip velocity of the flow at the stenosis throat as equation (7) and the velocity profile of the flow as equation (8) below.

$$U_\delta = \frac{p_x}{4\mu}\left[\frac{2R_a^2\ln\left(R_\delta/R\right) - \left(R_\delta^2 - R^2\right) + \pi\mu R_a^2\left(\left(R_a^2 - R^2\right)\ln\left(R_\delta/R\right) - \left(R_\delta^2 - R^2\right)\ln\left(R_a/R\right)\right)}{R_a\ln\left(R_\delta/R\right) + \frac{\pi\mu R_\delta R_a^2\sqrt{D_a}}{\alpha}\ln\left(R_a/R\right) + \frac{R_\delta\sqrt{D_a}}{\alpha}}\right] \tag{7}$$

$$U(r) = \frac{p_x}{4\mu}\left[r^2 - R^2 + \gamma R_a{}^2 \frac{\ln\left(r/R\right)}{\ln\left(R_\delta/R\right)} - \left(R_\delta{}^2 - R^2\right)\frac{\ln\left(r/R\right)}{\ln\left(R_\delta/R\right)}\right], \tag{8}$$

where

γ

$$= \left(\frac{R}{R_\delta}\right)\frac{2\left(\frac{R_a}{R}\right)^2 \ln\left(R_\delta/R\right) - \left(\left(\frac{R_\delta}{R}\right)^2 - 1\right) + \pi\mu R_a{}^2\left(\left(\left(\frac{R_a}{R}\right)^2 - 1\right)\ln\left(R_\delta/R\right) - \left(\left(\frac{R_\delta}{R}\right)^2 - 1\right)\ln\left(R_a/R\right)\right)}{\left(\frac{R_a}{R_\delta}\right)\ln\left(R_\delta/R\right) + \frac{\pi\mu R_a{}^2\sqrt{D_a}}{\alpha}\ln\left(R_a/R\right) + \frac{\sqrt{D_a}}{\alpha}}$$

Next we calculate the flux of the flow but in doing so we shall consider only the flux of the region of constriction and that of the ECM respectively. The part of the channel without any obstruction is considered the standard as it is assumed that the flow in those regions is free of any resistance. To get the flux we use the following equation adapted from [28]:

$$Q = 2\pi\left[\int_0^{R_\delta} rU dr + \int_{R_a}^{R} rU dr\right]. \tag{9}$$

By employing equation (8) in equation (9) and simplifying we obtain the flux of the flow as

Q

$$= \frac{\pi R^4 p_x}{8\mu}\left\{\begin{array}{l}\left(\frac{R_\delta}{R}\right)^4 + \left(\frac{R_a}{R}\right)^4 - 2\left[\left(\frac{R_\delta}{R}\right)^2 + \left(\frac{R_a}{R}\right)^2\right] + \frac{\beta}{R}\left(\frac{R_a}{R}\right)\left(\frac{R_\delta}{R}\right)\left[2\log\left(\frac{R_\delta}{R}\right) - 1\right] \\ \qquad + \frac{\beta}{R}\left(\frac{R_a}{R}\right)^3\left[2\log\left(\frac{R_a}{R}\right) - 1\right]\end{array}\right\}, \tag{10}$$

where $\dfrac{\beta}{R} = \dfrac{\pi R_a R_\delta \mu^2\sqrt{D_a}\left[\left(\frac{R_a}{R}\right)^2 - 1\right] - \alpha\left[\left(\frac{R_\delta}{R}\right)^2 - 1\right] - 2\left(\frac{R_a}{R}\right)\left(\frac{R_\delta}{R}\right)\mu\sqrt{D_a}}{\left(\frac{R_\delta}{R}\right)\sqrt{D_a} + \alpha\left(\frac{R_a}{R}\right)\log\left(\frac{R_\delta}{R}\right) - \left(\frac{R_a}{R}\right)^2 R R_\delta \pi\mu\sqrt{D_a}\log\left(\frac{R_a}{R}\right)}$.

From equation (10) we obtain the pressure gradient as

$$p_x = \frac{8\mu Q}{\pi R^4 \Gamma}, \tag{11}$$

where

$$\Gamma = \left(\frac{R_\delta}{R}\right)^4 + \left(\frac{R_a}{R}\right)^4 - 2\left[\left(\frac{R_\delta}{R}\right)^2 + \left(\frac{R_a}{R}\right)^2\right] + \frac{\beta}{R}\left(\frac{R_a}{R}\right)\left(\frac{R_\delta}{R}\right)\left[2\log\left(\frac{R_\delta}{R}\right) - 1\right] + \frac{\beta}{R}\left(\frac{R_a}{R}\right)^3\left[2\log\left(\frac{R_a}{R}\right) - 1\right].$$

Integrating (11) with respect to the variable x along the channel length L yields the pressure gradient as

$$\nabla p = \int_0^L p_x \, dx = \frac{8\mu Q}{\pi R^4}\Phi, \tag{12}$$

where

$$\Phi = \int_0^d \frac{1}{\Gamma}dx + \int_d^{d+\frac{l}{2}} \frac{1}{\Gamma}dx + \int_{d+\frac{l}{2}}^{d+l} \frac{1}{\Gamma}dx + \int_{d+l}^{\frac{3}{2}d+l} \frac{1}{\Gamma}dx + \int_{\frac{3}{2}d+l}^{\frac{3}{2}d+l+R_a} \frac{1}{\Gamma}dx + \int_{\frac{3}{2}d+l+R_a}^{\frac{3}{2}d+l+2R_a} \frac{1}{\Gamma}dx + \int_{\frac{3}{2}d+l+2R_a}^{L} \frac{1}{\Gamma}dx.$$

Evaluating the first, fourth and seventh integrals yields $L - l - 2R_a = L\left(1 - \frac{l + 2R_a}{L}\right)$, and with this the flow resistance in the stenosis region becomes

$$\bar{\lambda} = \frac{\nabla p}{Q} = \frac{8\mu}{\pi R_\delta^{\,4}}\left(\frac{L - l - 2R_a}{\Gamma} + \Theta\right), \tag{13}$$

where $\Theta = \frac{1}{L}\left[\int_{d}^{d+\frac{1}{2}} \frac{1}{\Gamma} dx + \int_{d+\frac{1}{2}}^{d+l} \frac{1}{\Gamma} dx + \int_{\frac{3}{2}d+l}^{\frac{3}{2}d+l+R_a} \frac{1}{\Gamma} dx + \int_{\frac{3}{2}d+l+R_a}^{\frac{3}{2}d+l+2R_a} \frac{1}{\Gamma} dx\right]$.

From equation (13), we obtain the non-dimensional form of flow resistance, as described in [7, 8, 26] from the stenosis region as

$$\lambda = \frac{\overline{\lambda}}{\lambda_0} = \Omega\left\{\frac{1-(l-2a)/L}{\Gamma_0} + \frac{1}{\Gamma_0}\Theta\right\}, \tag{14}$$

where $\lambda_0 = \frac{8\mu}{\Gamma_0 \pi R^4}$, $\Gamma_0 = \varepsilon^4 - 2\varepsilon^2 + \frac{\beta_0}{R}\left\{\varepsilon^3\left[\log(\varepsilon) - 1\right] - \varepsilon\right\} - 1$,

$\frac{\beta_0}{R} = \frac{\pi\mu^2\varepsilon\left(\varepsilon^2 - 1\right) - 2\frac{\mu\varepsilon}{R^2}}{\frac{1}{R^2} - \varepsilon^2\pi\mu\log(\varepsilon)}$, $\varepsilon = \frac{R_\delta}{R_a}$ and $\Omega = 2\left(2\mu^2 R^2 - 1\right)$.

Since our numeric result is in two parts we obtained the following expressions to be used in each of these regions. Expressions for the stenosis free region are with subscript 'a', whereas those for the ECM free regions are subscripted 'δ'.

ECM free region: $\frac{\beta_\delta}{R} = \frac{\pi R_a R_\delta \mu^2 \sqrt{D_a}\left[\varepsilon^2 - 1\right] - \alpha\left[\left(\frac{R_\delta}{R}\right)^2 - 1\right] - 2\varepsilon\left(\frac{R_\delta}{R}\right)\mu\sqrt{D_a}}{\frac{R_\delta}{R}\sqrt{D_a} + \alpha\varepsilon\log\left(\frac{R_\delta}{R}\right) - \varepsilon^2 R R_\delta \pi\mu\sqrt{D_a}\log(\varepsilon)}$ and

$\Gamma_\delta = \left(\frac{R_\delta}{R}\right)^4 + \left(\frac{R_\delta}{R}\right)^2 - 2\left[\left(\frac{R_\delta}{R}\right)^2 + \left(\frac{1}{\varepsilon}\right)^2\right] + \frac{\beta_\delta}{R}\varepsilon\left\{\left(\frac{R_\delta}{R}\right)^2\left[2\log\left(\frac{R_\delta}{R}\right) - 1\right] + \varepsilon^2\left[2\log(\varepsilon) - 1\right]\right\}$

Stenosis free region; $\frac{\beta_a}{R} = \frac{\pi R_a R \mu^2\left[\left(\frac{R_a}{R}\right)^2 - 1\right] - 2\left(\frac{R_a}{R}\right)\mu}{1 - \left(\frac{R_\delta}{R}\right)^2 R^2 \pi\mu\log\left(\frac{R_\delta}{R}\right)}$ and

$\Gamma_a = \left(\frac{R_a}{R}\right)^4 - 2\left(\frac{R_a}{R}\right)^2 - 1 + \frac{\beta_a}{R}\left(\frac{R_a}{R}\right)\left\{\left(\frac{R_a}{R}\right)^2\left[2\log\left(\frac{R_a}{R}\right) - 1\right] - 1\right\}$.

We also considered the hydraulic conductivity of the flow duct following the definition given in [18] and obtained the dimensionless hydraulic conductivity, L_p, as

$$L_p = \frac{1}{\lambda A}. \tag{15}$$

3. Numerical results and discussion

Because of the fact that solutions for the resistance and hydraulic conductivity is not possible analytically, we resorted to numerical solution approach. The flow channel is partitioned into two, the first is $0 \leq z_1 \leq 0.5$ and the second is $0.5 \leq z_2 \leq 1$. We assumed equal length for both ECM and stenosis and considered that d which locates the stenosis in the channel is zero. The first two integrals are evaluated with equations 1(a) and (b) respectively whereas 2(a) and (b) are used to evaluate the second and fourth integrals. We followed [3, 14] closely, in simulation and the numerical results, and obtained different results as presented and discussed in the figures shown below.

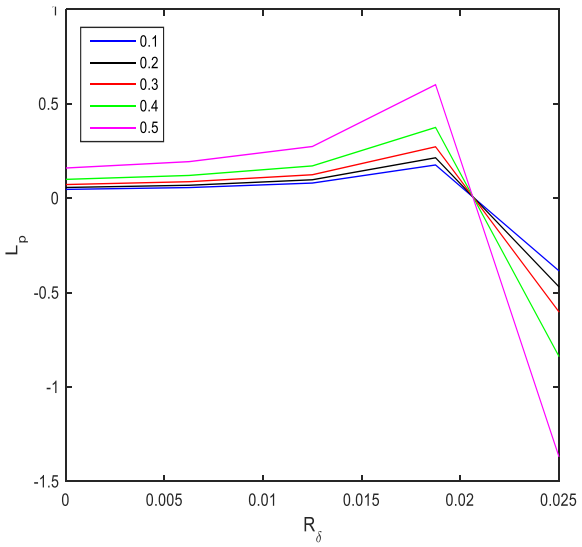

Figure 2: The effect of stenosis radius on Hydraulic conductivity with different varying slip paremeters.

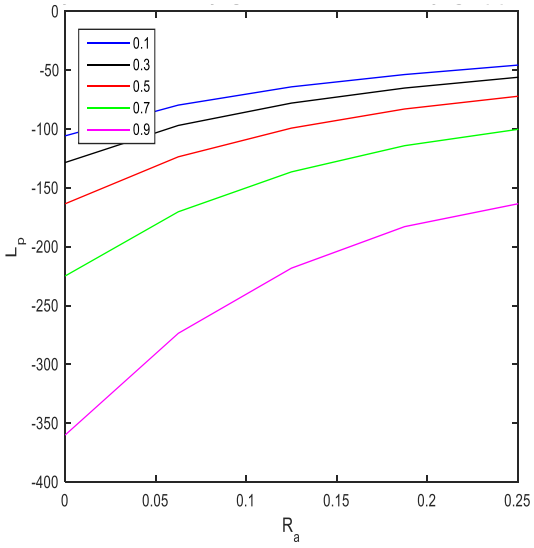

Figure 3: The relationship between Hydraulic conductivity and the ECM.

Figures 2 and 3 show that hydraulic conductivity increases in the presence of stenosis and ECM with varying slip parameter. On one hand, it increases with increasing slip parameter, gradually though, in the presence of stenosis until the flow starts to come just immediately after the stenosis throat when the hydraulic conductivity starts to decline in a reverse order with the slip parameter. This concept, as we think, may be due to the drag force caused by the presence of ECM in the flow profile.

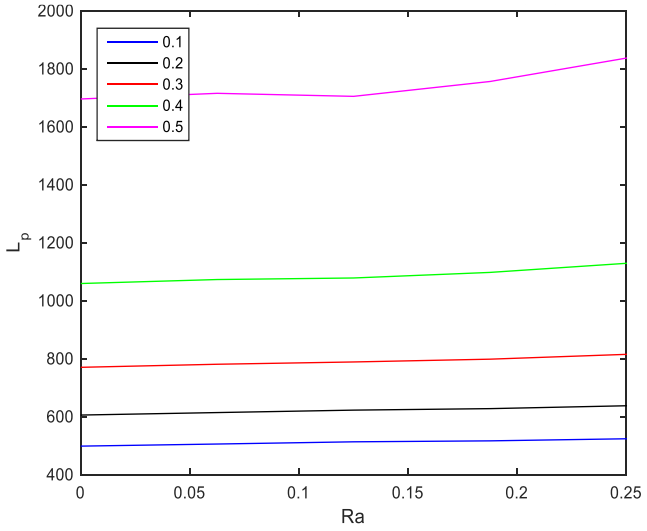

Figure 4. The effect of Darcy Number on Hydraulic conductivity and ECM.

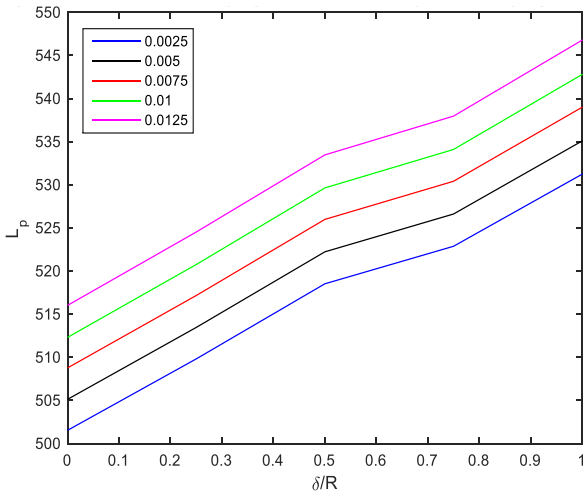

Figure 5. This shows how stenosis height affects Hydraulic conductivity in the presence of ECM.

In Figure 4 we see that the Hydraulic conductivity varies directly with the Darcy number in the presence of the ECM. As shown in this figure, the hydraulic conductivity of the flow gradually increases with higher Darcy number despite the increase in ECM diameter. It appears from this that the effect of Darcy number and the ECM cancel out each other, to some extent. This is open for further study. As is expected, Figure 5 shows that, in the presence of ECM, the stenosis height affects hydraulic conductivity. If a smaller area of the flow channel is under the influence of the drag from the ECM, the ease with which AH moves through the channel is lower than when a larger area is covered by the ECM. It then means that the presence of ECM contributes more pressure to the flow profile.

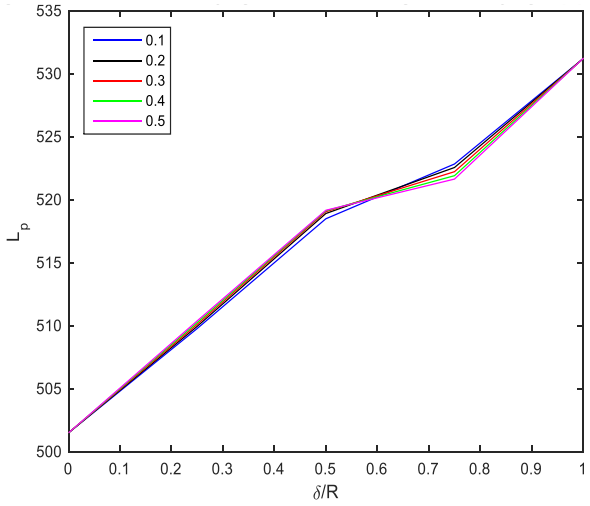

Figure 6. How Hydraulic conductivity behaves against stenosis height with varying slip parameters.

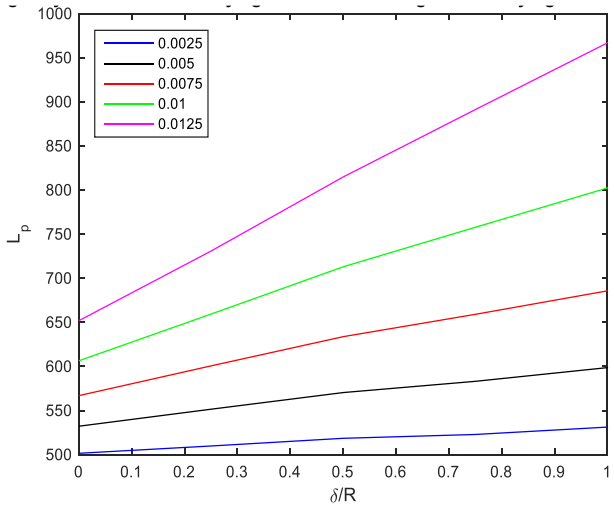

Figure 7. Display of how stenosis height affects Hydraulic conductivity in the varying stenosis radius.

Figure 6 shows that the slip parameters has little or no effect on the flow profile with respect to the Hydralc conductivity and the stenosis height. Nevertheless, it can be seen that the hadraulic conductivity responds directly to the stenosis with the slip parameter up to the mouth of the middle of the stenosis where the eefct of the slip is noticed. This is seen in the way the slip parameters switchs their positions, insignificantly though. From Figure 7, it is evident that the flow starts out with less ease due to, may be, the funneling effect caused by the pores considered as the stenosis but eases out as the flow moves out of the pores. It is also observable that with longer radii, the ease of flow through the pores increases. The effect of the stenosis is seen to delay hydraulic conductivity around the stenosis throat.

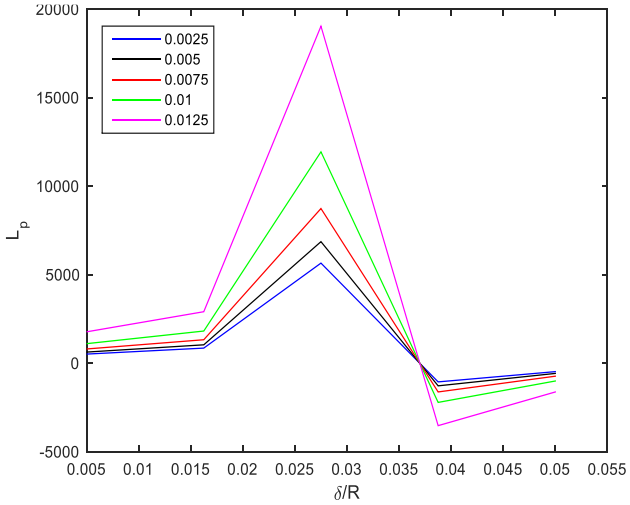

Figure 8. A display of effect of ECM on hydaraulic conductivity and stenosis radius.

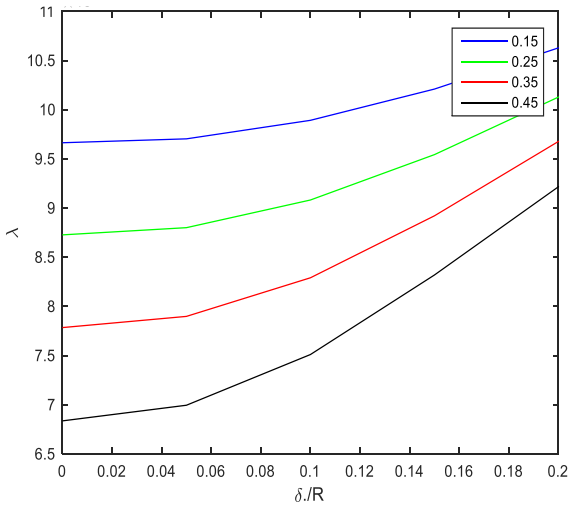

Figure 9. A plot showing the effect of stenosis height on Resistance in the presence of ECM.

Figure 8 displays the combined effect of stenosis and ECM on hydraulic conductivity. As is expected increase in ECM radius affects hydraulic conductivity of the flow. On the other hand, presence of stenosis is seen to affect hydraulic conductivity since it declines just immediately after the stenosis throat. Remarkable is Fgure 9 which shows how resistance is affected by ECM. It shows that increase in ECM radius increases the resistance. The steepness of the resistance profile is deeper with increasing ECM which agrees with our expectation.

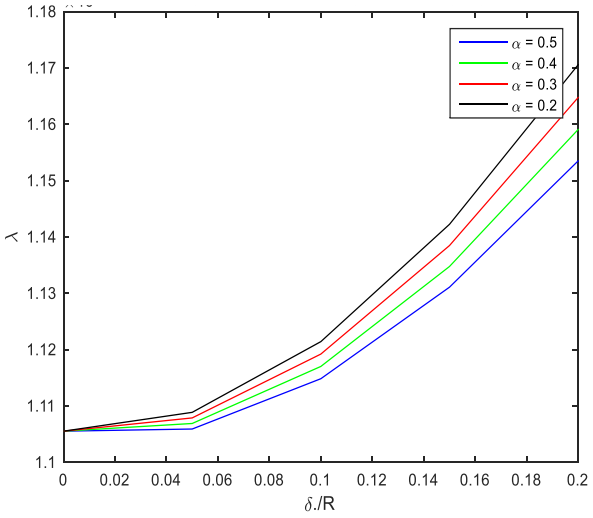

Figure 10. How resistance is affected by stenosis in the presence of different slip parameters.

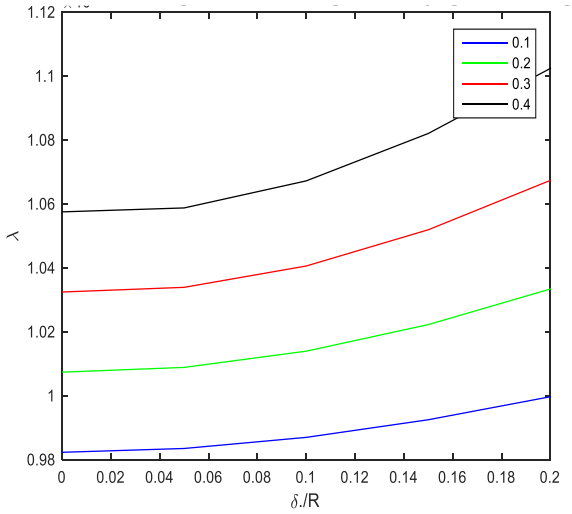

Figure 11. A plot of how stenosis height and radius affect resistance.

Figure 10 shows that resistance is increases with increasing stenosis height. However, the result is different in the presence of slip parameter. As can be seen from this figure, resistance decreases with higher slip parameter value but reduces otherwise. İt goes on to show the the role of slip parameter in the resistance profile of the flow through constriction. On the other hand, we see from Figure 11 that the height of the stenosis directly affects the resistance. İn other words, the more steep the constriction the more the resistance.

4. Conclusion

Based on these results from numeric solution and simulations we conclude that these structures affect the flow resistance and hydraulic conductivity, and might likely contribute to increase in IOP. We can then infer from the study that reducing the stenosis height can reduce resistance to AH flow, in addition to regulating ECM spread.

References

[1] Acott T.S. and Kelley M.J. (2008). Extracellular matrix in the trabecular meshwork. Exp. Eye Res., 86:543–61.

[2] Akbar S. and Shah S. (2020). The effects of prostaglandin analogs on intraocular pressure in human eye for open angle glaucoma. International Journal of Innovative Technology and Exploring Engineering, 10(2): 176 - 180.

[3] Avtar R., Srivastava S., and Srivastava R. (2014). Modelling the flow of aqueous humor in schlemm's canal in the eye. AAM: Intern. J., 9(1). http://pvamu.edu/aam.

[4] Avtar R. and Srivastava R. (2006). Modelling the flow of aqueous humor in anterior chamber of the eye. Applied Mathematics and Computation 181: 1336–1348.

[5] Avtar R. and Srivastava R. (2006). Aqueous outflow in Schlemms canal. Applied Mathematics and Computation 174 : 316–328.

[6] Bhatt K., Gong H., and Fredo T.F. (1995). Freeze-fracture studies of interendothelial junctions in the angle of the human eye. Invest Ophthalmol Vis Sci, 36(7):1379–1389.

[7] Bird R.B., Stewart W. E., and Lightfoot E.N. (2002). Transport Phenomena. John Wiley & Sons, Singapore, p97.

[8] Biswas D. and Chakraborty U.S. (2010). Pulsatile blood flow through a catheterized artery with an axially nonsymmetrical stenosis. Applied Mathematical Science, 4 (58); 2865-2880.

[9] Braunger B.M, Fuchshofer R., and Tamm E.R. (2015). The aqueous humor outflow pathways in glaucoma: A unifying concept of disease mechanisms and causative treatment. Eur J Pharm Biopharm, 95 (Pt B):173-81.

[10] David M. S. and Harry A. Q. (2004). Aqueous flow through the iris–lens channel: estimates of differential pressure between the anterior and posterior chambers. J. Glaucoma, 13: 100 – 107.

[11] Ethier C.R, Chan D.W., and Johnson M. (2001). Cationic ferritin changes outflow facility in human eyes whereas anionic ferritin does not. Invest Ophthalmol Vis Sci.; 42:1795–1802. [PubMed: 11431444].

[12] Ethier C.R. (2002). The inner wall of Schlemm's canal. Exp Eye Res. 74:161–172. [PubMed: 11950226].

[13] Ficarrotta K.R., Mohamed Y.H., and Passaglia C.L. (2020). Experimental glaucoma model with controllable intraocular pressure history. Natureresearch, 10:126. https://doi.org/10.1038/s41598-019-57022-5.

[14] Fitt A.D. (2008). Flow in the canal of schlemm and its influence on primary open angle glaucoma. In Bonilla, L.L., Moscoso, M., Platero, G. and Vega, J.M. (eds), Progress in Industrial Mathematics, Germany, Springer, 843-847.

[15] Fuchshofer R. and Tamm E.R. (2009). Modulation of extracellular matrix turnover in the trabecular meshwork. Exp Eye Res.; 88:683–688. [PubMed: 19385040].

[16] Goel M., Picciani R.G., Lee R.K., and Bhattacharya S.K. (2010). Aqueous humor dynamics: a review. The Open Ophthalmology Journal,Vol. 4, 52-59.

[17] Gottanka J., Chan D., Eichhorn M., and Johnson M. (2004). Effects of TGF-beta2 in perfused human eyes. Invest Ophthalmol Vis Sci;45:153-158.

[18] Grierson I. and Lee W.R. (1974). Junctions between the cells of the trabecular meshwork. Albrecht Von Graefes Arch Klin, Exp Ophthalmol, 192:89–104.

[19] Hann C.R., Bahler C.K., and Johnson D.H. (2005). Cationic ferritin and segmental flow through the trabecular meshwork. Invest. Ophthalmol Vis Sci.; 46(1):1-7.

[20] Johnson M. and Tamm E.R. (2010). Biomechanics of aqueous humor outflow resistance. Elsevier 2010 Adapted from Johnson, M. (2006), What controls aqueous humour outflow resistance? Experimental Eye Research, 82: 545–557.

[21] Johnson M. (2006). What controls aqueous humor outflow resistance? Exp Eye Res; 82:545–57.

[22] Maepea O. and Bill A. (1992). Pressures in the juxtacanalicular tissue and Schlemm's canal in monkeys. Exp Eye Res, 54(6): 879-883.

[23] Ngwu B.A., Iorkua M., Mmaduakor C.O., and Odafi O.N. (2018). Mathematical model of aqueous humour flow through a constricted channel. Journal of the Nigerian Association of Mathematical Physics, 47: 47 – 54.

[24] Overby D.R., Stamer W.D., and Johnson M. (2009). The changing paradigm of outflow resistance generation: towards synergistic models of the JCT and inner wall endothelium. Exp Eye Res., 88:656-670.

[25] Raviola G. and Raviola E. (1981). Paracellular route of aqueous outflow in the trabecular meshwork and canal of Schlemm. A freeze-fracture study of the endothelial junctions in the sclerocorneal angel of the macaque monkey eye. Invest Ophthalmol Vis Sci., 21:52–72.

[26] Shah S.R., Siddiqui S.U., and Sing A. (2016). Performance of blood flow through two phase stenosed artery using Herschel-Bulkley model. International Journal of Applied and Pure Science and Agriculture, 02(2): 228-240.

[27] Srivastav R.K. (2015). Mathematical model of blood flow through a composite stenosis in catheterized artery with permeable wall. Application and Applied Mathematics: An International Journal, 9(1): 58-74.

[28] Srivastav V.P., Vishnoi R., Sing D., Medhavi A., and Mishra S. (2015). Response to blood flow through an overlapping stenosis in catheterized arteries. E-Journal of Science and Technology, 5(6): 93-103.

[29] Tamm E.R., Braunger B.M., and Fuchshofer R. (2015). Chapter Eighteen - Intraocular pressure and the mechanisms involved in resistance of the aqueous humor flow in the trabecular meshwork outflow pathways, In 'Progress in Molecular Biology and Translational Science', Academic Press, Volume 134: 301-314.

[30] Tamm E.R. and Johnson M. (2009). The trabecular meshwork outflow pathways: structural and functional aspects. Exp Eye Res., 88: 648–655. PubMed: 19239914.

[31] Villamarina A., Roy S., Hasballa R., Vardoulis O., Reymond P., and Stergiopulos N. (2012). 3D simulation of the aqueous flow in the human eye. Journal of Medical Engineering and Physics 34; 1462 – 1470. www. elsevier.com/locate/medengphy.

[32] Vranka J.A., Kelley M.J., Acott T.S., and Keller K.E. (2015). Extracellular matrix in the trabecular meshwork: Intraocular pressure regulation and dysregulation in glaucoma. Exp Eye Res, 133: 112–125. doi:10.1016/j.exer.2014.07.014.

[33] Yuan N., Li M., Chen X., Lu Y., Fang Y., Gong H., Qian L., Wu J., Zhang S., Shipp S., Andolina I.M., Sun X., and Wang W. (2020). Immediate impact of acute elevation of intraocular pressure on cortical visual motion processing. Invest Ophthalmol Vis Sci., 61(5):59. https://doi.org/10.1167/iovs.61.5.59.